

# M3258 Is a Selective Inhibitor of the Immunoproteasome Subunit LMP7 ( $\beta 5i$ ) Delivering Efficacy in Multiple Myeloma Models



Michael P. Sanderson<sup>1</sup>, Manja Friese-Hamim<sup>1</sup>, Gina Walter-Bausch<sup>1</sup>, Michael Busch<sup>1</sup>, Stefanie Gaus<sup>1</sup>, Djordje Musil<sup>1</sup>, Felix Rohdich<sup>1</sup>, Ugo Zanelli<sup>1</sup>, Sondra L. Downey-Kopyscinski<sup>2</sup>, Constantine S. Mitsiades<sup>2</sup>, Oliver Schadt<sup>1</sup>, Markus Klein<sup>1</sup>, and Christina Esdar<sup>1</sup>

## ABSTRACT

Large multifunctional peptidase 7 (LMP7/ $\beta 5i$ /PSMB8) is a proteolytic subunit of the immunoproteasome, which is predominantly expressed in normal and malignant hematolymphoid cells, including multiple myeloma, and contributes to the degradation of ubiquitinated proteins. Described herein for the first time is the preclinical profile of M3258; an orally bioavailable, potent, reversible and highly selective LMP7 inhibitor. M3258 demonstrated strong antitumor efficacy in multiple myeloma xenograft models, including a novel model of the human bone niche of multiple

myeloma. M3258 treatment led to a significant and prolonged suppression of tumor LMP7 activity and ubiquitinated protein turnover and the induction of apoptosis in multiple myeloma cells both *in vitro* and *in vivo*. Furthermore, M3258 showed superior antitumor efficacy in selected multiple myeloma and mantle cell lymphoma xenograft models compared with the approved nonselective proteasome inhibitors bortezomib and ixazomib. The differentiated preclinical profile of M3258 supported the initiation of a phase I study in patients with multiple myeloma (NCT04075721).

## Introduction

The ubiquitin–proteasome system (UPS) plays an essential role in maintaining cellular homeostasis by degrading ubiquitinated proteins (1). The immunoproteasome and constitutive proteasome are multisubunit cylindrical complexes each containing three proteolytic subunits; large multifunctional peptidase 2 (LMP2/ $\beta 1i$ /PSMB9), MECL-1 (LMP10/ $\beta 2i$ /PSMB10), and LMP7 ( $\beta 5i$ /PSMB8) in the immunoproteasome, replaced, respectively, by  $\beta 1$  ( $\beta 1c$ /PSMB6),  $\beta 2$  ( $\beta 2c$ /PSMB7), and  $\beta 5$  ( $\beta 5c$ /PSMB5) in the constitutive proteasome (2). The unique cleavage specificity of each subunit enables degradation of diverse substrates and generates a broad repertoire of peptides for presentation on MHC class I (3). Unlike the ubiquitously expressed constitutive proteasome, the immunoproteasome is predominantly present in hematolymphoid cells (4, 5) and is typically only induced in

other cells by inflammatory stimuli-like IFN $\gamma$  (6). The immunoproteasome possesses a high capacity for degradation of oxidized, misfolded, and aggregated proteins to maintain homeostasis under acute cellular stress (7).

Multiple myeloma is a malignancy of monoclonal plasma cells, which reside in the bone marrow or extramedullary organs (8). Consistent with their hematopoietic origin, multiple myeloma cells predominantly express the immunoproteasome (4, 5). High expression of monoclonal immunoglobulin renders multiple myeloma cells acutely dependent on UPS components, including immunoproteasomes (9). The UPS also influences the malignancy of multiple myeloma cells by degrading specific tumor suppressors, proapoptotic proteins, and cell-cycle inhibitory proteins (10). The “pan-proteasome inhibitors” (pan-PIs) bortezomib, carfilzomib, and ixazomib, which target several immunoproteasome and constitutive proteasome subunits, are approved for use in patients with multiple myeloma (11). However, inhibition of the constitutive proteasome in healthy tissues is postulated to underly diverse toxicities associated with pan-PIs, including peripheral neuropathy, cardiac disorders, gastrointestinal disturbances, fatigue and thrombocytopenia, which can necessitate dose reductions or treatment discontinuation (12).

Selective immunoproteasome targeting has been proposed as a means of maintaining or improving upon the antitumor efficacy of pan-PIs in multiple myeloma, while circumventing severe dose-limiting toxicities (11). Although approved pan-PIs display unique properties (e.g., subunit preferences, reversibility, and administration route), they all potentially inhibit the immunoproteasome subunit LMP7 (9), suggesting that LMP7 is an important determinant of their efficacy. However, *in vivo* examination of the role of LMP7 in multiple myeloma models has been hampered by the lack of suitable LMP7 inhibitors, with previous reports only describing compounds retaining LMP2 or  $\beta 5$  inhibition or having properties precluding *in vivo* application (4, 13–18).

This study describes the profile of M3258—a potent, highly selective, reversible, and orally bioavailable LMP7 inhibitor. The robust efficacy of M3258 in diverse multiple myeloma models, including those that were refractory to bortezomib and/or ixazomib, supported

<sup>1</sup>Merck KGaA, Darmstadt, Germany. <sup>2</sup>Department of Medical Oncology, Dana-Farber Cancer Institute, Boston, Massachusetts.

**Note:** Supplementary data for this article are available at Molecular Cancer Therapeutics Online (<http://mct.aacrjournals.org/>).

C. Esdar, G. Walter-Bausch, and M. Friese-Hamim and M.P. Sanderson contributed equally as co-authors of this article.

Current address for U. Zanelli: Galderma SA, La Tour-de-Peilz, Switzerland; and current address for S.L. Downey-Kopyscinski: Rancho BioSciences, San Diego, CA.

**Corresponding Author:** Michael P. Sanderson, Merck KGaA, Frankfurter Strasse 250, Darmstadt, 64293, Germany. Phone: 49-615-1725-6970; Fax: 49-61-517-2914-9106; E-mail: michael.sanderson@merckgroup.com

Mol Cancer Ther 2021;20:1378–87

doi: 10.1158/1535-7163.MCT-21-0005

This open access article is distributed under Creative Commons Attribution-NonCommercial-NoDerivatives License 4.0 International (CC BY-NC-ND).

©2021 The Authors; Published by the American Association for Cancer Research

initiation of a phase I clinical trial of M3258 in patients with relapsed/refractory multiple myeloma (NCT04075721).

## Materials and Methods

### Compounds

M3258 was synthesized at Merck KGaA. The experimental method for preparation of M3258 is described previously in patent WO 2019/038250 (compound number 9; ref. 19). Bortezomib was purchased from ChemShuttle, Activate Scientific, and SelleckChem. Carfilzomib and ixazomib were sourced from ChemShuttle.

### Assessment of proteasome subunit binding and inhibition

Human immunoproteasomes (2  $\mu$ L used at 0.25 nmol/L), purified as described previously (20), or human constitutive proteasomes (Boston Biochem, used at 1.25 nmol/L) was preincubated for 2 hours at 25°C with 50 nL of compounds diluted in dimethyl sulfoxide (DMSO) in 20 mmol/L Tris pH 7.5, 0.03% sodium dodecyl sulfate (SDS) and 1 mmol/L ethylenediaminetetraacetic acid (EDTA). A total of 3  $\mu$ L of fluorogenic peptidic substrates (from Bachem Holding, unless stated otherwise) was added to the indicated final concentrations: 50  $\mu$ mol/L Ac-nLPnLD-AMC for  $\beta$ 1; 80  $\mu$ mol/L (Ac-PAL) 2R110 (Biomol) for LMP2; 20  $\mu$ mol/L Ac-RLR-AMC for  $\beta$ 2 and MECL-1; Suc-LLVY-AMC at either 40  $\mu$ mol/L for LMP7 or 50  $\mu$ mol/L for  $\beta$ 5. Fluorescence was measured using an Envision 2104 plate reader (PerkinElmer) following substrate addition and after 1 hour. Excitation and emission settings were used according to the substrate provider's instructions. The inhibitory activity of compounds was ascertained by calculating the difference in fluorescence at each time point. The IC<sub>50</sub> values were calculated by nonlinear regression analysis using Genedata Screener (Genedata).

The protocol for assessment of the reversibility of LMP7 inhibition by compounds and x-ray crystallography are described previously in the Supplementary Materials and Methods. The data collection and refinement statistics for the immunoproteasome-M3258 structure are shown in Supplementary Table S1.

### Cell lines and primary cells

Each cell line was obtained as frozen vials from Merck KGaA's internal cell bank that received original cells from the providers indicated in Supplementary Table S2. The internal cell bank generated master cell banks of each cell line and routinely performed the following quality control analyses: sterility testing, confirmation of the absence of *Mycoplasma* infection, identity testing by short tandem repeat analysis, and confirmation of the absence of cell line cross-contamination. For each experiment, cells were freshly thawed and passaged at least once before use. Cells were not used at passage numbers above 30 and were not cultured for more than 4 months.

Peripheral blood mononuclear cells (PBMCs) were isolated from lithium-heparinized blood by density gradient centrifugation using 50-mL Leucosep tubes (Greiner Bio One International) according to the manufacturer's instructions. Dog and rat PBMCs were isolated from lithium-heparinized blood. All rat and dog studies were performed in compliance with local government and European Union animal health and welfare guidelines.

### In vitro cellular assays

For cellular LMP7 and LMP2 activity assays, cell lines or rat PBMCs were seeded in 96-well plates at 10,000 cells per well, or 20,000 cells per well for human and dog PBMCs, in 100  $\mu$ L of PBS and cultured with compounds or DMSO for 2 hours. Fifty microliters of a lysis buffer of

100 mmol/L 4-(2-hydroxyethyl)-1-piperazineethanesulfonic acid (HEPES) pH 7.6, 60 mmol/L MgSO<sub>4</sub>, 1 mmol/L EDTA and 40  $\mu$ g/mL digitonin, supplemented with either the LMP7 substrate (Ac-ANW) 2R110 or LMP2 substrate (Ac-PAL)2R110 (both from Biomol and used at a final concentration of 10  $\mu$ mol/L), was then added to each well. Plates were shaken, incubated for 60 minutes at 37°C and then centrifuged at 300  $\times$  g. Fluorescence (excitation 485 nm, emission 535 nm) was measured and dose-response curves were plotted on the basis of the percentage of inhibition for each compound relative to DMSO. IC<sub>50</sub> values were calculated by nonlinear regression analysis using PRISM (GraphPad).

For assessment of cellular  $\beta$ 5 activity, human whole-blood samples were collected in citrate tubes (Becton Dickinson) and treated with compounds for 2 hours at 37°C. Samples were diluted 1:16 in PBS to reduce viscosity and 100  $\mu$ L was then transferred to black 96-well plates. Samples were lysed for 3 hours in the lysis buffer described previously above containing 10  $\mu$ mol/L (Suc-LLVY)2R110 before fluorescence measurement (excitation 494 nm and emission 521 nm).

To assess the effect of M3258 on MM.1S cell viability, 10,000 cells were seeded per well in 96-well plates and M3258 or DMSO added the following day. After 72 hours, 10- $\mu$ L resazurin (R&D Systems) was added and the plates were incubated for 3 hours before fluorescence measurement (excitation 531 nm and emission 590 nm). The effect of M3258 on caspase 3/7 activity in MM.1S cells was assessed using the Caspase-Glo 3/7 Assay System (Promega) according to the manufacturer's instruction. The effects of M3258 and ixazomib on primary human cells were assessed using the BioMAP Diversity PLUS Panel for Broad Phenotypic Profiling (Eurofins DiscoverX).

For assessment of the effect of M3258 on cellular ubiquitinated proteins levels, 40,000 MM.1S cells were seeded per well in 96-well plates and cultured overnight. Cells were incubated for 6 hours with M3258 or DMSO, then lysed for 20 minutes on ice in 25 mmol/L HEPES, 100 mmol/L NaCl, 29 mmol/L dodecyl-maltoside, and phosphatase inhibitor cocktail II and protease inhibitor cocktail set III (both from Merck KGaA). Lysates were transferred to Luminex measurement plates (Merck KGaA) and mixed overnight at 4°C with 2,000 microspheres coupled with an anti-ubiquitin (Lys48) antibody (clone 9H284; Biomol). The microspheres were then washed with an assay buffer of Blocking Reagent For ELISA (Roche Diagnostics) with 1% Tween 20 (Sigma-Aldrich), then mixed with the biotinylated mouse anti-ubiquitinated proteins antibody (clone FK1; Sigma-Aldrich) at 1  $\mu$ g/mL for 1 hour at room temperature. After further washing, the microspheres were mixed with the R-Phycoerythrin-conjugated streptavidin antibody (Dianova, 1:800 dilution) for 45 minutes at room temperature. The microspheres were then washed and resuspended in 120  $\mu$ L of assay buffer before measurement using a Luminex 200 instrument (Luminex) according to the manufacturer's instructions by counting 100 events per sample.

### In vivo tumor models

M3258 was dissolved in PBS containing 0.5% METHOCEL Premium K4M (Colorcon) and 0.25% Tween 20. Bortezomib was dissolved in 0.9% NaCl containing Mannitol (Merck KGaA) and ixazomib was dissolved in 5% KLEPTOSE (AppliChem).

All subcutaneous xenografts using human cell lines were established by injection of cells into the right-flanks of female H2d Rag2 mice (Taconic Biosciences) or female CB-17 SCID mice (Charles River Laboratories). 100  $\mu$ L of the following cell suspensions were injected per mouse: Granta-519, OPM-2, NCI-H929 and U266B1 at 5 million cells in PBS mixed 1:1 with Matrigel (Becton Dickinson); MM.1S at 5 million cells in PBS; RPMI 8226 at 10 million cells in PBS. Tumor

volume and mouse body weight were assessed twice weekly. The MTD was defined as the dose that did not cause mortality, >20% body weight loss or irreversible clinical or pathological findings. Statistical comparison of the efficacy of treatments was performed by repeated measures analysis of covariance (RM-ANCOVA).

The *in vivo* disseminated MM.1S and human osteoclast/scaffold-based MM.1S models were established as described previously (13, 21). Statistical assessment of the effect of M3258 on mouse survival in these models was performed using log-rank (Mantel–Cox) analyses.

Mouse studies at Merck KGaA were conducted according to protocols approved by the local governmental committee. Mice were housed under pathogen-free conditions in an AAALAC-accredited facility and treated according to the institutional, governmental and European Union guidelines (GV-SOLAS and FELASA). Mouse studies at Dana Farber Cancer Institute (DFCI) were conducted in accordance with the institutional animal care and use committee (IACUC) guidelines. Mice were housed in a pathogen-free environment at the DFCI animal facility and handled in strict accordance with Good Animal Practice as defined by the Office of Laboratory Animal Welfare.

#### Pharmacodynamic and pharmacokinetic analyses from *in vivo* studies

For pharmacodynamic (PD) analyses from xenograft tumors, between 50 and 100 mg of tumor tissue were lysed as described previously (22). LMP7 activity and ubiquitinated protein levels were assessed as described above. For assessment of caspase 3/7 activity, 50- $\mu$ g tumor lysate protein in 50  $\mu$ L was transferred to 96-well plates and mixed with the Caspase-Glo 3/7 Reagent (Promega) according to the manufacturer's instruction before luminescence measurement. Statistical analysis of PD data was performed using one-way ANOVA with Bonferroni's multiple comparison tests.

For Western blotting, tumor tissue was lysed in 10 mmol/L Tris-HCl pH 7.4, 150 mmol/L NaCl, 1% Nonidet P40, 1% Triton X-100, 0.4% deoxycholic acid sodium salt, 2 mmol/L EDTA and 0.3% SDS. Five to 10  $\mu$ g of protein was electrophoresed on NuPAGE 4% to 12% Bis-Tris Midi Protein Gels (Thermo Fisher Scientific) and transferred to Immuno-Blot LF PVDF membranes (Bio-Rad). Blocking was performed using Odyssey Blocking Buffer (LI-COR). The sources of Western blotting antibodies are shown in Supplementary Table S3.

The protocols for pharmacokinetic (PK) assessment of M3258, bortezomib, and ixazomib from mouse *in vivo* studies are described in the Supplementary Materials and Methods.

## Results

### M3258 structure and LMP7 binding and inhibition

The structure of M3258 is shown in Fig. 1A. The x-ray structure of the human 20S immunoproteasome is shown in Fig. 1B. Co-crystallization studies with the human immunoproteasome and M3258 suggested a covalent bond between threonine-1 of the human LMP7 catalytic site and the M3258 boron (Fig. 1C). The benzofuran moiety fills the lipophilic S1 pocket of LMP7 and contributes to the selectivity of M3258. The adjacent amide group is essential for activity by forming a hydrogen bond with serine-21. The attached bicyclic ether moiety of M3258 is positioned such that the ether-oxygen forms a highly specific hydrogen bond with the peptide backbone (alanine-49) of the LMP7 subunit. The discovery of M3258, guided by structure-based optimization and balancing of properties enabling oral bioavailability, will be described in a separate publication (M. Klein; unpublished data). M3258, bortezomib, and ixazomib demonstrated 68%, 20%, and 53% mean reversibility of human LMP7 inhibition after 1 hour, respectively, indicative of a reversible inhibition mechanism (Supplementary Table S4). In contrast, carfilzomib demonstrated 3%

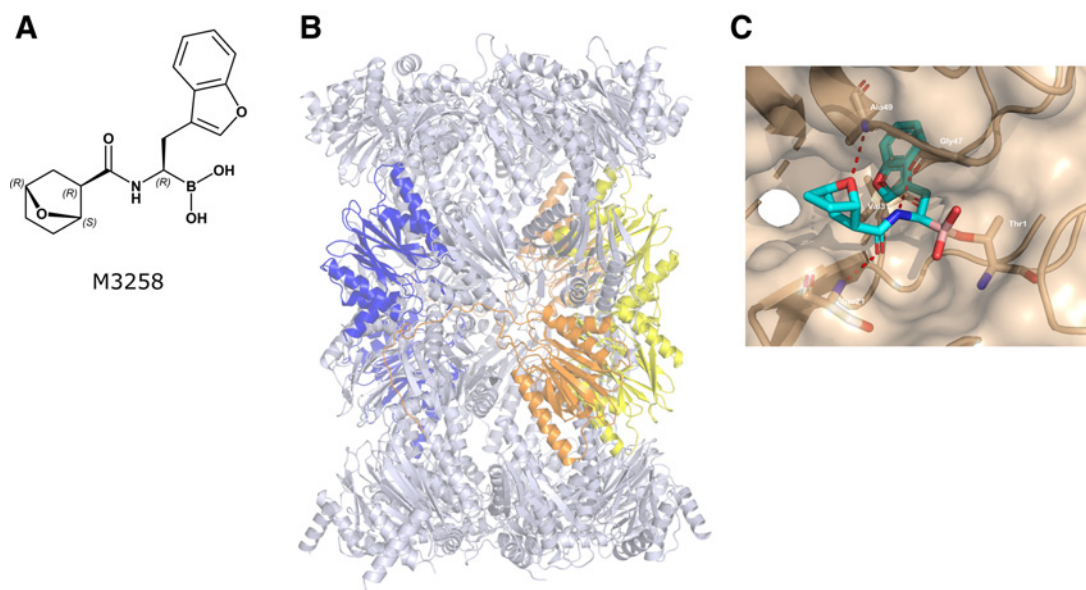


**Figure 1.**

M3258 chemical structure and human LMP7 binding. **A**, The chemical structure of M3258 is indicated. The labels *R* and *S* indicate the absolute configuration of the respective M3258 stereocenters. **B**, The x-ray structure of the human 20S immunoproteasome particle is indicated. LMP2, LMP7, and MECL-1 are shown in yellow, blue, and orange, respectively. The x-ray structure data can be found in the Protein Data Bank (PDB) under the identification code 7awe. **C**, The x-ray structure of M3258 bound to the catalytic site of human LMP7 (marked brown) at a resolution of 2.78 Å. Hydrogen bonds between LMP7 and M3258 are indicated by red dashed lines.

**Table 1.** Inhibition of proteasome subunits by M3258, bortezomib, carfilzomib, and ixazomib.

	Constitutive proteasome subunits			Immunoproteasome subunits		
	$\beta$ 1	Mean IC <sub>50</sub> (nmol/L) $\pm$ SD (n)		LMP2	MECL-1	LMP7
		$\beta$ 2	$\beta$ 5			
M3258	>30,000 (4)	>30,000 (4)	2,519 $\pm$ 397 (5)	>30,000 (5)	>30,000 (4)	4.1 $\pm$ 2.4 (5)
Bortezomib	18 $\pm$ 10 (7)	13,358 $\pm$ 5,331 (8)	3.0 $\pm$ 1.1 (14)	1.6 $\pm$ 1.8 (8)	1,653 $\pm$ 482 (11)	0.9 $\pm$ 0.3 (12)
Carfilzomib	451 $\pm$ 380 (3)	46 $\pm$ 19 (3)	2.3 $\pm$ 1.0 (4)	41 $\pm$ 17 (4)	15 $\pm$ 7.0 (3)	3.3 $\pm$ 1.1 (5)
Ixazomib	28 $\pm$ 22 (4)	>30,000 (4)	5.5 $\pm$ 2.3 (4)	0.9 $\pm$ 0.2 (4)	5,469 $\pm$ 1,095 (3)	3.3 $\pm$ 3.0 (4)

Note: The inhibition of the indicated proteolytic subunits of the constitutive proteasome and immunoproteasome was determined in cell-free biochemical assays. For each assay, mean IC<sub>50</sub> values (nmol/L)  $\pm$  SD and the number of replicates (n) are indicated. Abbreviation: SD, standard deviation.

mean reversibility, consistent with an irreversible mechanism. Together, these data indicate that M3258 is a covalent-reversible LMP7 inhibitor: a mechanism shared by bortezomib and ixazomib (23), but distinct from the covalent-irreversible drug carfilzomib (24).

The inhibitory activity of M3258, bortezomib, carfilzomib, and ixazomib toward each human immunoproteasome and constitutive proteasome proteolytic subunit was assessed using cell-free peptide cleavage assays. M3258 inhibited human LMP7 with a mean IC<sub>50</sub> value of 4.1 nmol/L (Table 1). At the highest tested concentration of 30,000 nmol/L, M3258 did not demonstrate 50% inhibition of the immunoproteasome subunits LMP2 and MECL-1 or the constitutive proteasome subunits  $\beta$ 1 and  $\beta$ 2. M3258 displayed weak activity against the constitutive proteasome subunit  $\beta$ 5 (mean IC<sub>50</sub> = 2,519 nmol/L). These data indicate that M3258 has high potency and >600-fold selectivity for LMP7. PK/PD modeling, to be described in a separate publication (F. Lignet; unpublished data), predicted the efficacious dose range of M3258 in human to deliver a total plasma maximum concentration (C<sub>max</sub>) range of 2,090 to 5,550 nmol/L. When corrected for plasma protein binding (fraction unbound in human = 2.7%), the corresponding predicted unbound M3258 C<sub>max</sub> range (56 to 150 nmol/L) is between 16- and 44-fold below the mean M3258 IC<sub>50</sub> value for  $\beta$ 5. Bortezomib, carfilzomib, and ixazomib inhibited LMP7 with comparable potency to M3258, but consistent with previous reports (23, 24) also potentially inhibited other constitutive proteasome and immunoproteasome subunits (Table 1).

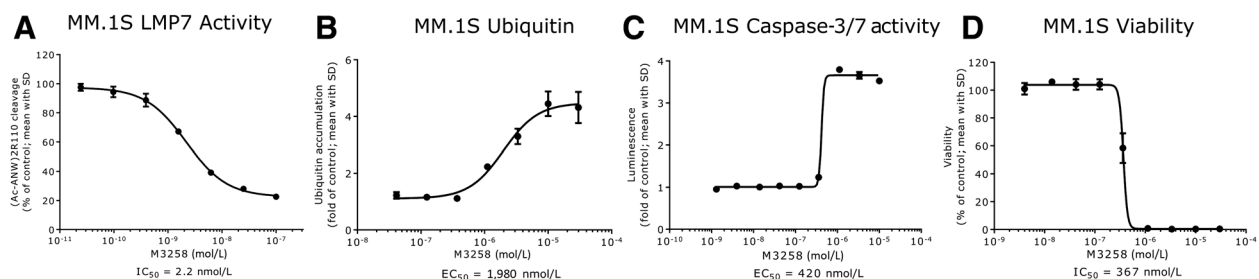
#### Inhibition of cellular LMP7, LMP2, and $\beta$ 5 activity

Cellular LMP7 activity was assessed using the fluorogenic peptidic substrate (Ac-ANW)2R110, previously described to be cleaved by LMP7 (25). M3258 potently inhibited LMP7 in the human multiple myeloma cell lines MM.1S and U266B1 and in human, rat, and dog

PBMCs with IC<sub>50</sub> values between 2 and 37 nmol/L (Fig. 2A; Supplementary Fig. S1A–S1D). Bortezomib, carfilzomib, and ixazomib inhibited LMP7 in U266B1 cells with comparable potency to M3258 (Supplementary Fig. S1A). The maximal inhibition (E<sub>max</sub>) of (Ac-ANW)2R110 cleavage by M3258 in cells was between 58% and 92%, which was lower than that for the pan-PIs. This suggests that although LMP7 is the predominant cellular protease that processes (Ac-ANW)2R110, residual cleavage is mediated by the remaining proteolytic targets of pan-PIs.

At concentrations up to 30,000 nmol/L, M3258 did not demonstrate 50% inhibition of LMP7 in the mouse B lymphoblast cell line P3X63Ag8.653 (Supplementary Fig. S1E). In contrast, bortezomib displayed comparable potency of LMP7 inhibition in this mouse cell line (IC<sub>50</sub> = 5.3 nmol/L) and cells from other species. This weaker activity of M3258 toward mouse LMP7 could be explained by the presence of a bulky methionine-31 in mouse LMP7 (substituted by valine in human LMP7, as indicated in Fig. 1C, and also in rat and dog LMP7), which was previously described to sterically hinder interaction with partially selective LMP7 inhibitors, while still accommodating bortezomib binding (26).

M3258 did not inhibit cleavage of the LMP2 substrate (Ac-PAL)2R110 in the human multiple myeloma cell line RPMI 8226 (Supplementary Fig. S1F), meanwhile in this same cell line LMP7 activity was potently inhibited (IC<sub>50</sub> = 4.4 nmol/L; Supplementary Fig. S1G). In contrast, bortezomib displayed comparable potency against both LMP2 activity (IC<sub>50</sub> = 7.3 nmol/L) and LMP7 activity (IC<sub>50</sub> = 2.3 nmol/L) in RPMI 8226 cells. The substrate (Suc-LLVY)2R110 was used to monitor cellular  $\beta$ 5 activity in human whole blood, as described previously (27). M3258 and bortezomib inhibited  $\beta$ 5 with IC<sub>50</sub> values of 13,700 and 268 nmol/L, respectively (Supplementary Fig. S1H). This M3258 IC<sub>50</sub> value is 2.5- to 6-fold higher than the

**Figure 2.**

*In vitro* PD effects of M3258 in the multiple myeloma cell line MM.1S. **A**, LMP7 activity in MM.1S cells treated with M3258 for 2 hours. **B**, Levels of ubiquitinated proteins in lysates from MM.1S treated for 6 hours with M3258. **C**, Induction of caspase 3/7 activity in MM.1S cells treated with M3258 for 72 hours. **D**, Effect of M3258 on the viability of MM.1S cells cultured for 96 hours. For each assay, IC<sub>50</sub> or EC<sub>50</sub> values (both in nmol/L) are indicated.

predicted efficacious total plasma  $C_{max}$  range for M3258 in humans, described previously above (2,090 to 5,550 nmol/L; F. Lignet; unpublished data). Together these data confirm the greatly increased selectivity of M3258 toward LMP7 compared with pan-PIs.

### ***In vitro* effects of M3258 on MM.1S cells and primary human cells**

Treatment of MM.1S cells *in vitro* with M3258 induced a >fourfold accumulation of ubiquitinated proteins with an  $EC_{50}$  value of 1,980 nmol/L (Fig. 2B), confirming that M3258 interfered with immunoproteasome function. M3258 also induced apoptosis as assessed by caspase 3/7 activity ( $EC_{50}$  = 420 nmol/L; >3.5-fold induction; Fig. 2C) and reduced MM.1S cell viability ( $IC_{50}$  = 367 nmol/L;  $E_{max}$  = 100%; Fig. 2D). The potency values in the apoptosis and viability assays corresponded to an M3258 concentration range that was associated with maximal inhibition of LMP7 activity in MM.1S cells (see Fig. 2A), suggesting that complete target coverage may be required to realize efficacy of selective LMP7 inhibitors. The comparatively high  $EC_{50}$  value in the ubiquitinated-protein accumulation assay may potentially reflect differences in the sensitivity or duration of each assay, or the involvement of proteasomal components beyond LMP7 in the turnover of cellular ubiquitinated proteins (28).

The effects of M3258 and ixazomib on human primary cells were assessed using the *in vitro* BioMAP Diversity PLUS Panel for Broad

Phenotypic Profiling. M3258 was tested up to 1,000 nmol/L in each assay, which is higher than the predicted human efficacious unbound M3258  $C_{max}$  range described previously above (56 to 150 nmol/L; F. Lignet; unpublished data). M3258 was not cytotoxic toward any primary human cell type at any concentration tested (Supplementary Fig. S2A). The M3258 profile indicated reduced proliferation of B cells (110, 330 and 1,000 nmol/L) and T cells (1,000 nmol/L). M3258 also reduced IL-2, IL-6, IL-17, IL-17F, TNF $\alpha$ , and IgG secretion by human PBMCs. All other primary human cell types and assay readouts were unaffected by M3258. In contrast, ixazomib was cytotoxic toward primary human B cells, PBMCs, mononuclear cells, and venular endothelial cells (33 nmol/L; Supplementary Fig. S2B). At a non-cytotoxic ixazomib concentration of 11 nmol/L, reduced proliferation of primary human coronary artery smooth muscle cells, endothelial cells, fibroblasts, and T cells was observed.

### **M3258 PK and PD effects in multiple myeloma xenograft studies**

Following a single application orally, M3258 dose-dependently reduced LMP7 activity in U266B1 xenograft tumors in mice (Fig. 3A). Maximal inhibition of LMP7 activity was sustained for  $\geq 24$  hours at M3258 doses of 10 and 30 mg/kg. Consistent with *in vitro* data in U266B1 cells described previously above (see Supplementary Fig. S1A), M3258 did not completely reduce (Ac-ANW)2R110 cleavage in U266B1 tumors. A dose-dependent increase in M3258 exposure

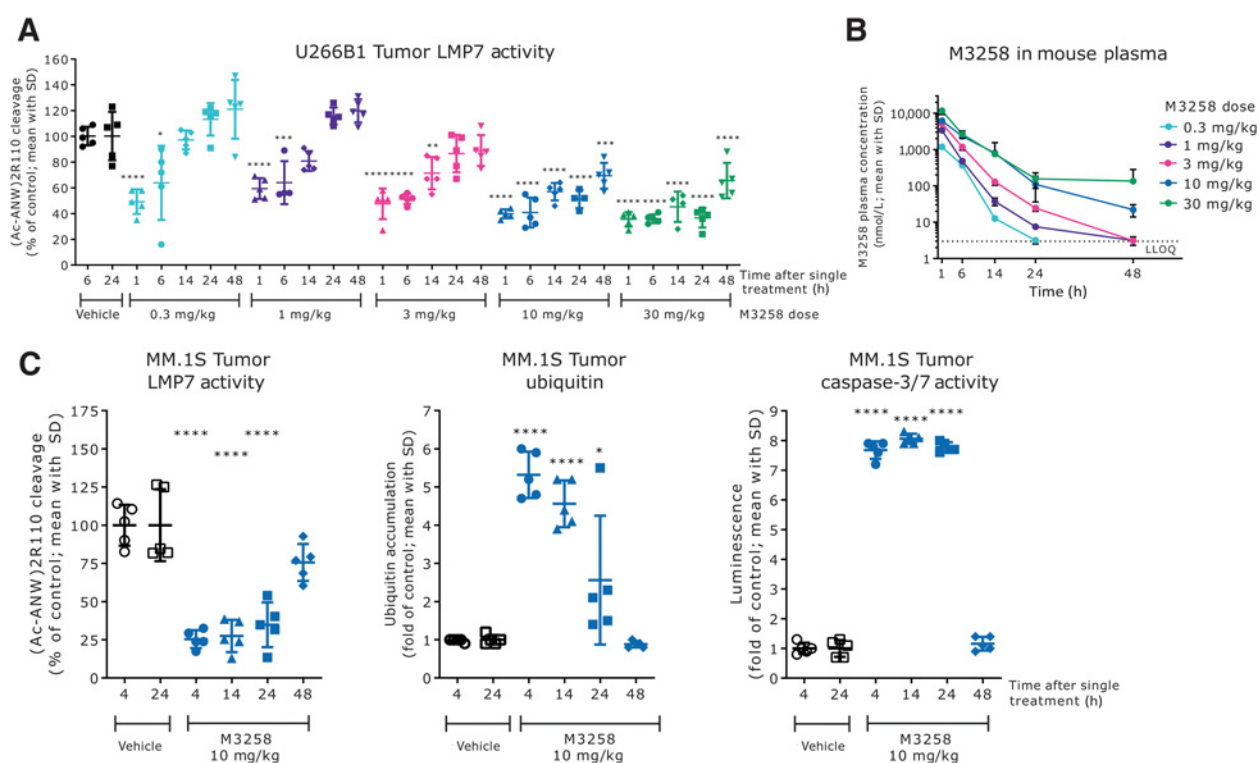


**Figure 3.**

*In vivo* PK and PD effects of M3258 in multiple myeloma xenograft models. **A**, Inhibition of LMP7 activity in subcutaneous U266B1 tumors from mice treated once with vehicle or M3258 at 0.3, 1, 3, 10 or 30 mg/kg orally. Statistical comparisons of LMP7 activity data were performed as follows: M3258 groups at 1, 6, and 14 hours versus vehicle at 6 hours; M3258 groups at 24 and 48 hours versus vehicle at 24 hours. **B**, Mouse plasma PK profiles for the indicated doses of M3258 from the experiment described in **A**. The lower limit of quantitation (LLOQ) for M3258 is indicated by the horizontal dashed line. **C**, LMP7 activity (left), levels of ubiquitinated proteins (middle), and caspase 3/7 activity (right) in subcutaneous MM.1S human multiple myeloma xenograft tumors from mice treated once orally with either vehicle or M3258 (10 mg/kg). Statistical comparisons of PD data were performed as follows: M3258 groups at 4 and 14 hours versus vehicle at 4 hours; M3258 groups at 24 and 48 hours versus vehicle at 24 hours. \*,  $P < 0.05$ ; \*\*,  $P < 0.01$ ; \*\*\*,  $P < 0.001$ ; \*\*\*\*,  $P < 0.0001$ .

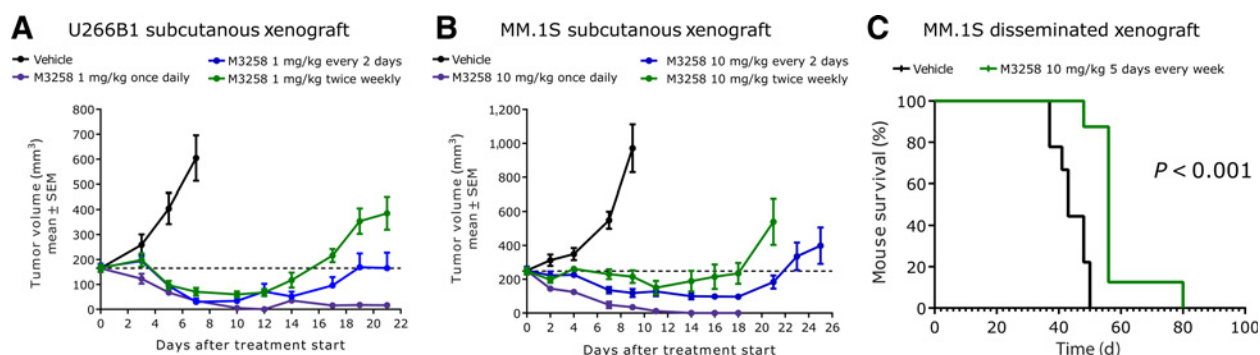


**Figure 4.**

*In vivo* efficacy of M3258 in subcutaneous and disseminated multiple myeloma xenograft models. **A**, Antitumor efficacy of M3258 at 1 mg/kg orally applied either once daily, every 2 days or twice weekly (days 1 and 4) in the U266B1 subcutaneous xenograft model. **B**, Antitumor efficacy of M3258 at 10 mg/kg orally applied either once daily, every 2 days or twice weekly (days 1 and 4) in the MM.1S subcutaneous xenograft model. For **A** and **B**, the percentage tumor/control (% T/C) values for each treatment and the statistical comparison of the efficacy of each group are shown in Supplementary Table S5. **C**, Mice bearing disseminated MM.1S cells, established via tail vein injection, were treated with M3258 (10 mg/kg, orally, 5 consecutive days of treatment every week) or vehicle and the percentage mouse survival was assessed. The *P* value for the statistical comparison of survival curves of the vehicle and M3258 groups is indicated.

in mouse plasma was observed in this study (Fig. 3B). M3258 did not affect LMP7 abundance in U266B1 tumors, meanwhile the constitutive proteasome subunit  $\beta 5$  was only increased at the highest tested dose of 30 mg/kg (Supplementary Fig. S3).

A single application of M3258 at 10 mg/kg orally significantly suppressed LMP7 activity and led to a significant accumulation of ubiquitinated protein levels in MM.1S tumors between 4 and 24 hours (Fig. 3C). A significant increase of caspase 3/7 activity was observed between 4 and 24 hours, indicating apoptosis induction. At 48 hours, each of these readouts was no longer significantly affected.

#### ***In vivo* efficacy of M3258 in multiple myeloma xenograft models**

When applied once daily at 1 mg/kg orally, M3258 displayed significant and strong antitumor efficacy, exemplified by sustained regression, in the U266B1 xenograft model (Fig. 4A; Supplementary Table S5), meanwhile intermittent schedules were associated with initial tumor regression followed by regrowth under treatment. Comparable findings were observed in the MM.1S xenograft model when using M3258 at 10 mg/kg orally (Fig. 4B; Supplementary Table S5).

The M3258 doses of 1 and 10 mg/kg were tolerated either when applied daily or intermittently (Supplementary Fig. S4A and S4B), confirming that the observed antitumor efficacy of M3258 at these doses was not due to adverse tolerability effects in mice. In a separate experiment, M3258 daily oral doses of 20 and 30 mg/kg were associated with mouse body weight loss in the range of 5% to 10%, which immediately recovered when pausing treatment for 2 days (Supplementary Fig. S4C). Together, these data suggest that the MTD of M3258 in mice, when applied daily, is 10 mg/kg. As shown above in Fig. 3B, the M3258 dose of 30 mg/kg led to a mean total plasma  $C_{max}$  in mice of 11,672 nmol/L, which is in a comparable range with the M3258  $IC_{50}$  value for  $\beta 5$  activity in whole blood (13,700 nmol/L; see Supplementary Fig. S1H), suggesting that the mouse body weight loss observed at this dose may potentially be due to  $\beta 5$  inhibition. The greatly reduced potency of M3258 against LMP7 in mouse cells compared with human, rat, and dog cells precluded the use of mice for assessment of on-target tolerability. Nonclinical safety studies, to be described in a separate publication (W. Sloot; unpublished data), indicated that rats and dogs tolerated repeated daily oral application of M3258 at doses delivering equivalent exposure to that at the mouse efficacious dose (10 mg/kg, once daily orally).

The antitumor activity of M3258 was next examined in mouse models recapitulating the pathogenesis and tumor environment of human multiple myeloma. In a disseminated model, generated via tail vein-injection of MM.1S cells, M3258 significantly prolonged median mouse survival by 13 days compared with the vehicle (Fig. 4C). In a model recapitulating the bone marrow environment of human multiple myeloma (model establishment depicted in Fig. 5A), M3258 treatment resulted in a significant and pronounced (110 days) prolongation of median mouse survival (Fig. 5B) and a delay of tumor growth (Fig. 5C).

#### **Comparative efficacy of M3258, bortezomib, and ixazomib in xenograft models**

The antitumor efficacy of M3258, bortezomib, and ixazomib was compared *in vivo*. Bortezomib was applied by intravenous injection twice weekly at 0.5 mg/kg, whereas ixazomib was applied twice weekly at 3 mg/kg orally. These doses and regimens were established as the mouse MTDs for bortezomib and ixazomib (Supplementary Fig. S5A–S5D). In addition, PK analyses from mice treated with bortezomib or ixazomib at these doses indicated that plasma exposures were reached in mice that were in a comparable range with that reported for humans treated with these agents at their approved doses (ref. 29; Supplementary Table S6).

In the U266B1 multiple myeloma model, both M3258 (10 mg/kg, once daily orally) and ixazomib induced prolonged complete tumor regression, even following treatment cessation (Fig. 6A; Supplementary Table S7). The strong efficacy observed with ixazomib is consistent with a previous preclinical report that also used this compound on a twice weekly treatment regimen (30). In this experiment, M3258 and ixazomib were significantly more efficacious than bortezomib. M3258 also displayed significant efficacy in the MM.1S and NCI-H929 multiple myeloma models, which was significantly higher than that with bortezomib, but not ixazomib (Supplementary Fig. S6A–S6C; Supplementary Table S8). Consistent with a previous report (31), bortezomib inhibited tumor growth in the RPMI 8226 multiple myeloma model (Fig. 6B; Supplementary Table S7). In this experiment, M3258 displayed equivalent efficacy to bortezomib, which was significantly greater than ixazomib. Intriguingly, the efficacy of M3258 in the OPM-2 multiple myeloma and the Granta-519 mantle cell lymphoma models was significantly greater than that observed with

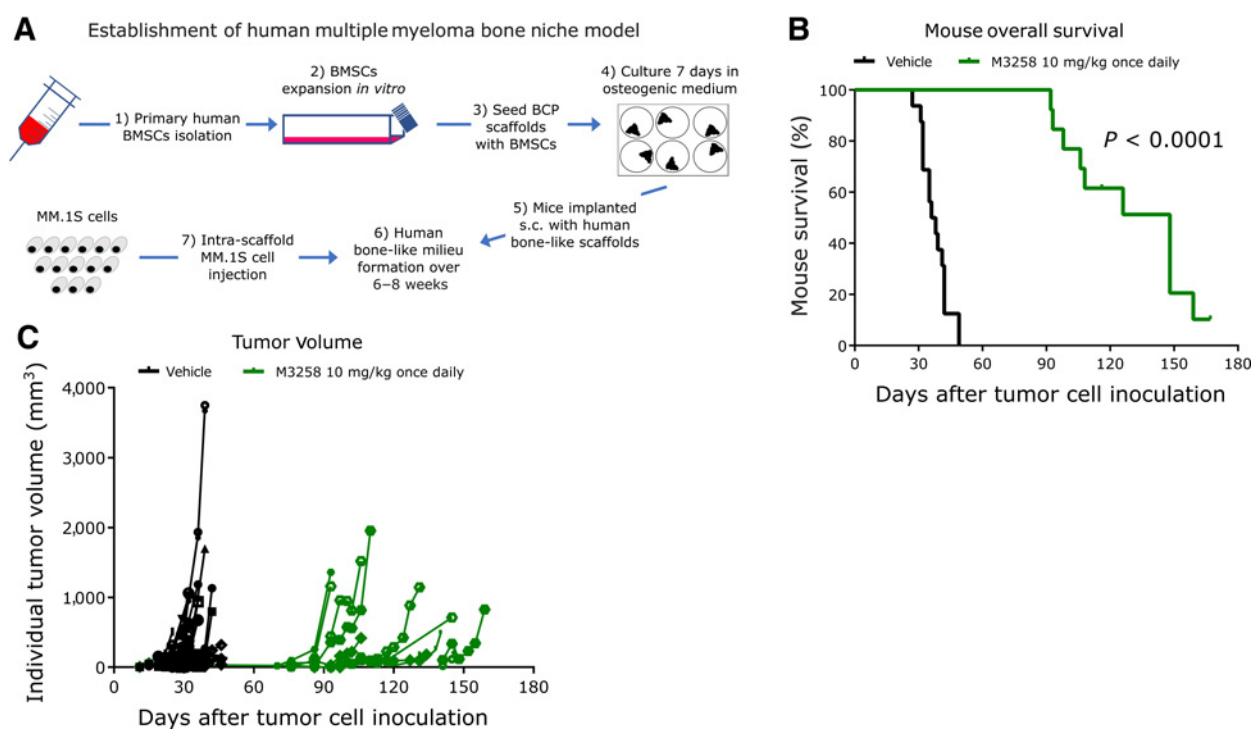


**Figure 5.**

*In vivo* efficacy of M3258 in a scaffold-based model of the human bone marrow niche. **A**, Representation of the establishment of the *in vivo* ceramic scaffold model of the human multiple myeloma bone marrow niche. Overall survival (**B**) and tumor volume (**C**) in mice bearing the MM.1S-containing scaffolds that were treated with vehicle or M3258 (10 mg/kg, once daily orally). The *P* value for the statistical comparison of survival curves of the vehicle and M3258 groups is indicated. Abbreviations: BCP, biphasic calcium phosphate; BMSC, bone marrow-derived stem cells; s.c., subcutaneous.

both bortezomib and ixazomib (Fig. 6C–D; Supplementary Table S7). Together, these data suggest that selective LMP7 inhibition delivers noninferior or even improved preclinical antitumor efficacy compared with bortezomib and ixazomib.

## Discussion

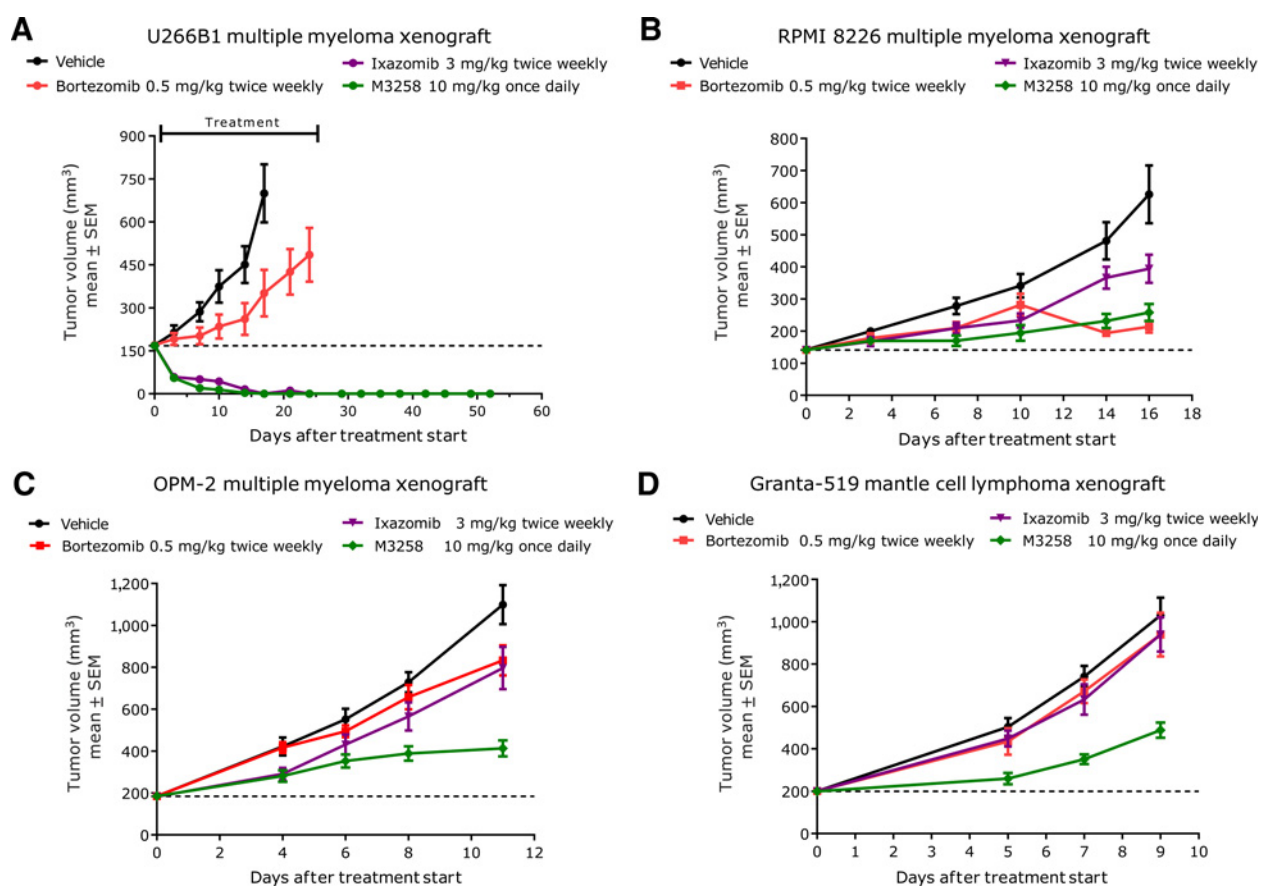
Since the initial approval of bortezomib, novel proteasome inhibitors with differentiated features, such as irreversible target binding (32), oral bioavailability (33) or brain penetration (34), have emerged and in some cases, these newer agents have fulfilled unmet needs of patients with multiple myeloma with regards to efficacy, selected safety limitations and/or convenience. Nevertheless, all proteasome inhibitors that are either approved or under clinical investigation in patients with multiple myeloma target multiple subunits of both the immunoproteasome and constitutive proteasome. This nonselective mechanism, particularly constitutive proteasome inhibition, is postulated to be associated with severe toxicities that limit the utility of these agents (11, 35). As such, novel proteasome inhibitors with improved features are of high interest for multiple myeloma and other diseases.

Because of the lack of highly selective LMP7 inhibitors with features enabling *in vivo* application, preclinical analysis of the function of LMP7 in multiple myeloma could previously only be performed via genetic targeting approaches *in vitro*. These published studies (36, 37) and publicly available gene dependency datasets (e.g., DepMap, <https://depmap.org>) suggested that the constitutive proteasome subunit  $\beta 5$  (gene name *PSMB5*) is essential for multiple myeloma cell lines and diverse other cell lines *in vitro*, whereas immunoproteasome proteolytic subunits, including LMP7 (gene name *PSMB8*), are dis-

pensable. These findings, together with reports describing that cell lines with acquired *in vitro* resistance to pan-PIs commonly harbor gatekeeper  $\beta 5$  mutations that impair drug binding (37–39), have implicated  $\beta 5$  targeting as a critical determinant of pan-PI efficacy. However, the rare frequency of such  $\beta 5$  mutations in patients with pan-PI-relapsed multiple myeloma brings into question the relevance of these *in vitro* findings (40–42). Furthermore, genetic ablation or alteration of LMP7 in cells has been described to alter diverse aspects of proteasome structure and function such as assembly, subunit maturation, and composition and thus may not represent the optimal approach for investigation of the proteolytic function of LMP7 in multiple myeloma (43–46).

The unique selectivity and *in vivo* PK properties of M3258 enabled us to demonstrate for the first time that multiple myeloma cells are highly dependent on LMP7 function *in vivo*, as exemplified by strong regression in several multiple myeloma tumor models and pronounced activity in models recapitulating the pathogenesis and tumor environment of human multiple myeloma. Furthermore, M3258 was associated with a long duration of antitumor efficacy, even following treatment cessation, suggesting that selective LMP7 blockade is not rapidly compensated by the activity of remaining proteasome subunits or other adaptive mechanisms.

Daily M3258 application was associated with more durable *in vivo* efficacy in multiple myeloma models compared with intermittent schedules. This can likely be explained by the necessity for continuous LMP7 suppression for sustained apoptosis induction and disruption of ubiquitinated protein turnover in multiple myeloma tumor cells. In contrast, published clinical studies suggest that the efficacy of pan-PIs is associated with the short-term suppression of the activity of multiple

**Figure 6.**

Comparison of the *in vivo* efficacy of M3258, ixazomib, and bortezomib in xenograft models. Mice bearing subcutaneous tumors derived from the human multiple myeloma cell lines U266B1 (A), RPMI 8226 (B) or OPM-2 (C) or the human mantle cell lymphoma cell line Granta-519 (D) were treated with vehicle, M3258 (10 mg/kg, once daily orally), bortezomib (0.5 mg/kg, twice weekly intravenously on days 1 and 4) or ixazomib (3 mg/kg, twice weekly orally on days 1 and 4). For A–D, the percentage of T/C values for each treatment and the statistical comparison of the efficacy of each group are shown in Supplementary Table S7.

proteasome subunits for only a few hours of each dosing cycle (27, 47). Our findings with M3258 suggest that unlike pan-PIs, selective LMP7 inhibitors may require tailored regimens, guided by their PK and PD profiles, to achieve the prolonged target suppression necessary for optimal activity.

Among the *in vivo* models we tested, M3258 demonstrated noninferior efficacy compared with bortezomib and ixazomib. Meanwhile, M3258 demonstrated elevated efficacy compared with these pan-PIs in the multiple myeloma model, OPM-2 and mantle cell lymphoma model, Granta-519. The OPM-2 model harbors the t(4;14) translocation (48), which is present in approximately 15% of newly diagnosed patients with multiple myeloma and predicts poor prognosis and a high-risk of progression from smoldering myeloma to multiple myeloma (8, 49). These findings suggest that selective LMP7 inhibition may represent an attractive strategy in patients with high-risk multiple myeloma, or patients that are resistant or refractory to pan-PIs.

M3258 delivered different degrees of *in vivo* efficacy across the tested multiple myeloma tumor models. The U266B1 model was uniquely sensitive to M3258 with sustained tumor regression observed at 1 and 10 mg/kg, which contrasted with the delayed tumor growth or stasis observed in other models treated with M3258 at 10 mg/kg. The finding that M3258 inhibited cellular LMP7 activity across multiple

myeloma cell lines in a comparable potency range suggests that the varying *in vivo* sensitivity of different multiple myeloma models to M3258 is likely due to determinants beyond the degree of target inhibition. Intriguingly, bortezomib and ixazomib also displayed differential degrees of efficacy across the tested multiple myeloma models. This was unexpected given the comparable proteasome subunit inhibition profiles of bortezomib and ixazomib, as well as the application of both compounds at their mouse MTDs. To our knowledge, our report is the most comprehensive preclinical comparison of the *in vivo* antitumor efficacy profiles of bortezomib and ixazomib. This dataset provides a basis for future investigation of the molecular determinants that underpin the differential responsiveness of multiple myeloma models to selective LMP7 inhibitors and individual pan-PIs.

Consistent with the predominant expression of LMP7 in tissues of hematolymphoid origin (4, 5), M3258 inhibited proliferation of primary human B and T cells. In contrast, ixazomib was cytotoxic toward these primary human cell types and others. Mouse models were not applicable for the direct *in vivo* comparison of the tolerability of M3258 and pan-PIs, due to the reduced activity of M3258 toward mouse LMP7. The results from nonclinical safety studies in rats and dogs, to be described in a separate publication (W. Sloot; unpublished data), identified only hematolymphoid tissues and the intestine (dog



only) as M3258 target organs, which contrasts with the broader spectrum of target organs for pan-PIs in nonclinical safety studies.

In summary, the unique profile of M3258 enabled us to demonstrate the exquisite dependency of multiple myeloma cells on LMP7 function *in vivo*. Selective LMP7 inhibition is a novel and differentiated mechanism for targeting multiple myeloma cells and represents a potentially attractive therapeutic strategy in this disease. Our preclinical observations supported the initiation a phase I study of M3258 as a single agent (dose-escalation) and co-administered with dexamethasone (dose-expansion) in patients with relapsed/refractory multiple myeloma (NCT04075721). Monitoring of LMP7 and  $\beta 5$  activity in patients receiving M3258 is planned in this trial to gain insights into the clinical utility of selective LMP7 inhibition in multiple myeloma.

### Authors' Disclosures

M.P. Sanderson reports a patent for LMP7-selective inhibitors for the treatment of blood disorders and solid tumors pending to Merck KGaA, Darmstadt, Germany, and reports employment with and is a stockholder of Merck, KGaA, Darmstadt, Germany. M. Friese-Hamim reports employment with Merck, KGaA, Darmstadt, Germany. G. Walter-Bausch reports a patent for LMP7-selective inhibitors for the treatment of blood disorders and solid tumors pending to Merck KGaA, Darmstadt, Germany, and reports employment with and is a stockholder of Merck, KGaA, Darmstadt, Germany. M. Busch reports employment with and is a stockholder of Merck, KGaA, Darmstadt, Germany. S. Gaus reports employment with and is a stockholder of Merck, KGaA, Darmstadt, Germany. D. Musil reports personal fees from Merck KGaA during the conduct of the study and is a stockholder of Merck, KGaA, Darmstadt, Germany. U. Zanelli reports personal fees from Merck KGaA during the conduct of the study. S.L. Downey-Kopyscinski reports other support from Merck KGaA, Darmstadt, Germany, during the conduct of the study as well as other support from Rancho BioSciences outside the submitted work. C.S. Mitsiades reports grants from Merck KGaA/EMD Serono during the conduct of the study as well as grants from Sanofi, Arch Oncology, AbbVie, Karyopharm, Janssen/Johnson & Johnson, TEVA, Nurix, H3 Biosciences, and personal fees from Fate Therapeutics, Ionis Pharmaceuticals, FIMECS, and other support from Takeda outside the submitted work. O. Schadt reports personal fees from Merck KGaA, Darmstadt, Germany, during the conduct of the study and has a patent for WO2019038250 pending to Merck KGaA, Darmstadt, Germany, and is a stockholder of Merck KGaA, Darmstadt, Germany. M. Klein reports a patent for WO2019038250 issued and a patent for LMP7-selective inhibitors for the treatment of blood disorders and solid tumors pending and reports employment from and is a stockholder of Merck, KGaA, Darmstadt, Germany. C. Esdar reports a patent for WO2019038250 issued to Merck KGaA, Darmstadt, Germany,

and a patent for LMP7-selective inhibitors for the treatment of blood disorders and solid tumors pending to Merck KGaA, Darmstadt, Germany, as well as reports employment with and is a stockholder of Merck KGaA, Darmstadt, Germany. No disclosures were reported by the other authors.

### Authors' Contributions

**M.P. Sanderson:** Conceptualization, resources, formal analysis, supervision, investigation, writing—original draft, project administration, writing—review and editing. **M. Friese-Hamim:** Conceptualization, formal analysis, supervision, investigation, methodology, writing—review and editing. **G. Walter-Bausch:** Conceptualization, formal analysis, supervision, investigation, methodology, writing—review and editing. **M. Busch:** Formal analysis, Investigation, writing—review and editing. **S. Gaus:** Formal analysis, Investigation, methodology. **D. Musil:** Formal analysis, supervision, investigation, methodology, writing—review and editing. **F. Rohdich:** Formal analysis, supervision, project administration, writing—review and editing. **U. Zanelli:** Formal analysis, supervision, project administration, writing—review and editing. **S.L. Downey-Kopyscinski:** Conceptualization, formal analysis, investigation, methodology, writing—review and editing. **C.S. Mitsiades:** Conceptualization, resources, formal analysis, investigation, methodology, project administration, writing—review and editing. **O. Schadt:** Conceptualization, formal analysis, supervision, investigation, project administration, writing—review and editing. **M. Klein:** Conceptualization, formal analysis, supervision, investigation, project administration. **C. Esdar:** Conceptualization, resources, formal analysis, supervision, investigation, project administration, writing—review and editing.

### Acknowledgments

This study was financially supported by Merck KGaA, Darmstadt, Germany. We acknowledge the support and contributions of the following people: Andreas Becker, Andree Blaukat, Julie DeMartino, Hugues Dolgos, Elise Drouin, Samer El Bawab, Ralf Emmerich, Claude Gimmi, Samantha Goodstal, Philipp Haselmayer, Hendrik Hollmann, Frank Jähring, Dilafuz Juraeva, Mirek Jurzak, Stephanie Karl, Mireille Krier, Daniel Kuhn, Long Li, Floriane Lignet, Laura Liu, Jianguo Ma, Felix Neumann, Pia Sanfelice, Melanie Schwarz, Willem Sloot, Sofia Stinchi, Heinz Thoma, Klaus Urbahns, Anja Victor, Ping Yu, Lars zur Brügge. We also acknowledge the contribution of Proteros Biostructures GmbH.

The costs of publication of this article were defrayed in part by the payment of page charges. This article must therefore be hereby marked *advertisement* in accordance with 18 U.S.C. Section 1734 solely to indicate this fact.

Received January 4, 2021; revised March 5, 2021; accepted May 7, 2021; published first May 27, 2021.

### References

- Micale N, Scarbaci K, Troiano V, Ettari R, Grasso S, Zappala M. Peptide-based proteasome inhibitors in anticancer drug design. *Med Res Rev* 2014;34:1001–69.
- Murata S, Takahama Y, Kasahara M, Tanaka K. The immunoproteasome and thymoproteasome: functions, evolution and human disease. *Nat Immunol* 2018; 19:923–31.
- Groettrup M, Kirk CJ, Basler M. Proteasomes in immune cells: more than peptide producers? *Nat Rev Immunol* 2010;10:73–8.
- Singh AV, Bandi M, Aujay MA, Kirk CJ, Hark DE, Raje N, et al. PR-924, a selective inhibitor of the immunoproteasome subunit LMP-7, blocks multiple myeloma cell growth both *in vitro* and *in vivo*. *Br J Haematol* 2011;152:155–63.
- Altun M, Galardy PJ, Shringarpure R, Hideshima T, LeBlanc R, Anderson KC, et al. Effects of PS-341 on the activity and composition of proteasomes in multiple myeloma cells. *Cancer Res* 2005;65:7896–901.
- Hallermalm K, Seki K, Wei C, Castelli C, Rivoltini L, Kiessling R, et al. Tumor necrosis factor- $\alpha$  induces coordinated changes in major histocompatibility class I presentation pathway, resulting in increased stability of class I complexes at the cell surface. *Blood* 2001;98:1108–15.
- A Habib J, De Plaen E, Stroobant V, Zivkovic D, Bousquet MP, Guillaume B, et al. Efficiency of the four proteasome subtypes to degrade ubiquitinated or oxidized proteins. *Sci Rep* 2020;10:15765.
- Sonneveld P, Avet-Loiseau H, Lonial S, Usmani S, Siegel D, Anderson KC, et al. Treatment of multiple myeloma with high-risk cytogenetics: a consensus of the International Myeloma Working Group. *Blood* 2016;127:2955–62.
- Kubiczkova L, Pour L, Sedlarikova L, Hajek R, Sevcikova S. Proteasome inhibitors—molecular basis and current perspectives in multiple myeloma. *J Cell Mol Med* 2014;18:947–61.
- Wallington-Beddoe CT, Sobieraj-Teague M, Kuss BJ, Pitson SM. Resistance to proteasome inhibitors and other targeted therapies in myeloma. *Br J Haematol* 2018;182:11–28.
- Ettari R, Zappala M, Grasso S, Musolino C, Innao V, Allegra A. Immunoproteasome-selective and non-selective inhibitors: a promising approach for the treatment of multiple myeloma. *Pharmacol Ther* 2018;182:176–92.
- Schlafer D, Shah KS, Panjic EH, Lonial S. Safety of proteasome inhibitors for treatment of multiple myeloma. *Expert Opin Drug Saf* 2017;16: 167–83.
- Downey-Kopyscinski S, Daily EW, Gautier M, Bhatt A, Florea BI, Mitsiades CS, et al. An inhibitor of proteasome beta2 sites sensitizes myeloma cells to immunoproteasome inhibitors. *Blood Adv* 2018;2:2443–51.
- Niewerth D, Franke NE, Jansen G, Assaraf YG, van Meerloo J, Kirk CJ, et al. Higher ratio immune versus constitutive proteasome level as novel indicator of sensitivity of pediatric acute leukemia cells to proteasome inhibitors. *Haematologica* 2013;98:1896–904.
- Niewerth D, Kaspers GJ, Assaraf YG, van Meerloo J, Kirk CJ, Anderl J, et al. Interferon- $\gamma$ -induced upregulation of immunoproteasome subunit assembly overcomes bortezomib resistance in human hematological cell lines. *J Hematol Oncol* 2014;7:7.

16. Koerner J, Brunner T, Groettrup M. Inhibition and deficiency of the immunoproteasome subunit LMP7 suppress the development and progression of colorectal carcinoma in mice. *Oncotarget* 2017;8:50873–88.
17. Ettari R, Pallio G, Pizzino G, Irrera N, Zappala M, Maiorana S, et al. Non-covalent immunoproteasome inhibitors induce cell-cycle arrest in multiple myeloma MM.1R cells. *J Enzyme Inhib Med Chem* 2019;34:1307–13.
18. Yeo JJ, Lee MJ, Baek A, Miller Z, Bhattarai D, Baek YM, et al. A dual inhibitor of the proteasome catalytic subunits LMP2 and Y attenuates disease progression in mouse models of Alzheimer's disease. *Sci Rep* 2019;9:18393.
19. Klein M, Schadt O, Estdar C. inventors; Merck Patent GmbH, assignee. Boronic acid derivatives. WO 2019/038250. 2019.
20. Dechavanne V, Vilbois F, Glez L, Antonsson B. Purification and separation of the 20S immunoproteasome from the constitutive proteasome and identification of the subunits by LC-MS. *Protein Expr Purif* 2013;87:100–10.
21. Groen RW, Noort WA, Raymakers RA, Prins HJ, Aalders L, Hofhuis FM, et al. Reconstructing the human hematopoietic niche in immunodeficient mice: opportunities for studying primary multiple myeloma. *Blood* 2012;120:e9–e16.
22. Buchstaller HP, Anlauf U, Dorsch D, Kuhn D, Lehmann M, Leuthner B, et al. Discovery and optimization of 2-arylquinazolin-4-ones into a potent and selective tankyrase inhibitor modulating Wnt pathway activity. *J Med Chem* 2019;62:7897–909.
23. Kupperman E, Lee EC, Cao Y, Bannerman B, Fitzgerald M, Berger A, et al. Evaluation of the proteasome inhibitor MLN9708 in preclinical models of human cancer. *Cancer Res* 2010;70:1970–80.
24. Kuhn DJ, Chen Q, Voorhees PM, Strader JS, Shenk KD, Sun CM, et al. Potent activity of carfilzomib, a novel, irreversible inhibitor of the ubiquitin-proteasome pathway, against preclinical models of multiple myeloma. *Blood* 2007;110:3281–90.
25. Santos RLA, Bai L, Singh PK, Murakami N, Fan H, Zhan W, et al. Structure of human immunoproteasome with a reversible and noncompetitive inhibitor that selectively inhibits activated lymphocytes. *Nat Commun* 2017;8:1692.
26. Huber EM, Heinemeyer W, de Bruin G, Overkleef HS, Groll M. A humanized yeast proteasome identifies unique binding modes of inhibitors for the immunosubunit beta5i. *EMBO J* 2016;35:2602–13.
27. Lee SJ, Levitsky K, Parlati F, Bennett MK, Arastu-Kapur S, Kellerman L, et al. Clinical activity of carfilzomib correlates with inhibition of multiple proteasome subunits: application of a novel pharmacodynamic assay. *Br J Haematol* 2016;173:884–95.
28. Wu HQ, Baker D, Ovaia H. Small molecules that target the ubiquitin system. *Biochem Soc Trans* 2020;48:479–97.
29. Liston DR, Davis M. Clinically relevant concentrations of anticancer drugs: a guide for nonclinical studies. *Clin Cancer Res* 2017;23:3489–98.
30. Park J, Park E, Jung CK, Kang SW, Kim BG, Jung Y, et al. Oral proteasome inhibitor with strong preclinical efficacy in myeloma models. *BMC Cancer* 2016;16:247.
31. LeBlanc R, Catley LP, Hideshima T, Lentzsch S, Mitsiades CS, Mitsiades N, et al. Proteasome inhibitor PS-341 inhibits human myeloma cell growth *in vivo* and prolongs survival in a murine model. *Cancer Res* 2002;62:4996–5000.
32. McBride A, Klaus JO, Stockerl-Goldstein K. Carfilzomib: a second-generation proteasome inhibitor for the treatment of multiple myeloma. *Am J Health Syst Pharm* 2015;72:353–60.
33. Richardson PG, Kumar S, Laubach JP, Paba-Prada C, Gupta N, Berg D, et al. New developments in the management of relapsed/refractory multiple myeloma—the role of ixazomib. *J Blood Med* 2017;8:107–21.
34. Badros A, Singh Z, Dhakal B, Kwok Y, MacLaren A, Richardson P, et al. Marizomib for central nervous system-multiple myeloma. *Br J Haematol* 2017;177:221–5.
35. Cengiz Seval G, Beksac M. The safety of bortezomib for the treatment of multiple myeloma. *Expert Opin Drug Saf* 2018;17:953–62.
36. Shi CX, Zhu YX, Bruins LA, Bonolo de Campos C, Stewart W, Braggio E, et al. Proteasome subunits differentially control myeloma cell viability and proteasome inhibitor sensitivity. *Mol Cancer Res* 2020;18:1453–64.
37. Basler M, Groettrup M. Recent insights how combined inhibition of immunoproteasome subunits enables therapeutic efficacy. *Genes Immun* 2020;21:273–87.
38. Franke NE, Niewerth D, Assaraf YG, van Meerloo J, Vojtekova K, van Zantwijk CH, et al. Impaired bortezomib binding to mutant beta5 subunit of the proteasome is the underlying basis for bortezomib resistance in leukemia cells. *Leukemia* 2012;26:757–68.
39. Oerlemans R, Franke NE, Assaraf YG, Cloos J, van Zantwijk I, Berkers CR, et al. Molecular basis of bortezomib resistance: proteasome subunit beta5 (PSMB5) gene mutation and overexpression of PSMB5 protein. *Blood* 2008;112:2489–99.
40. Barrio S, Stuhmer T, Da-Via M, Barrio-Garcia C, Lehnert N, Besse A, et al. Spectrum and functional validation of PSMB5 mutations in multiple myeloma. *Leukemia* 2019;33:447–56.
41. Lichter DI, Danaee H, Pickard MD, Tayber O, Sintchak M, Shi H, et al. Sequence analysis of beta-subunit genes of the 20S proteasome in patients with relapsed multiple myeloma treated with bortezomib or dexamethasone. *Blood* 2012;120:4513–6.
42. Politou M, Karadimitris A, Terpos E, Kotsianidis I, Apperley JF, Rahemtulla A. No evidence of mutations of the PSMB5 (beta-5 subunit of proteasome) in a case of myeloma with clinical resistance to Bortezomib. *Leuk Res* 2006;30:240–1.
43. Kunjappu MJ, Hochstrasser M. Assembly of the 20S proteasome. *Biochim Biophys Acta* 2014;1843:2–12.
44. Joeris T, Schmidt N, Ermert D, Krienke P, Visekruna A, Kuckelkorn U, et al. The proteasome system in infection: impact of beta5 and LMP7 on composition, maturation and quantity of active proteasome complexes. *PLoS One* 2012;7:e39827.
45. Arima K, Kinoshita A, Mishima H, Kanazawa N, Kaneko T, Mizushima T, et al. Proteasome assembly defect due to a proteasome subunit beta type 8 (PSMB8) mutation causes the autoinflammatory disorder, Nakajo-Nishimura syndrome. *Proc Natl Acad Sci U S A* 2011;108:14914–9.
46. Kitamura A, Maekawa Y, Uehara H, Izumi K, Kawachi I, Nishizawa M, et al. A mutation in the immunoproteasome subunit PSMB8 causes autoinflammation and lipodystrophy in humans. *J Clin Invest* 2011;121:4150–60.
47. Assouline SE, Chang J, Cheson BD, Rifkin R, Hamburg S, Reyes R, et al. Phase 1 dose-escalation study of IV ixazomib, an investigational proteasome inhibitor, in patients with relapsed/refractory lymphoma. *Blood Cancer J* 2014;4:e251.
48. Moreaux J, Klein B, Bataille R, Descamps G, Maiga S, Hose D, et al. A high-risk signature for patients with multiple myeloma established from the molecular classification of human myeloma cell lines. *Haematologica* 2011;96:574–82.
49. Pawlyn C, Morgan GJ. Evolutionary biology of high-risk multiple myeloma. *Nat Rev Cancer* 2017;17:543–56.